

# Room-temperature continuous-wave operation of InGaAsSb/AlGaAsSb quantum-well diode lasers emitting at 2.3 $\mu$ m

ZHAN GUO LI, MING HUI YOU<sup>a,\*</sup>, XIN GAO, GUOJUN LIU, ZHONG LIANG QIAO, LIN LI, YI QU, BAO XUE BO, XIAO HUI MA

*National Key Laboratory on High Power Semiconductor Lasers, Changchun University of Science and Technology, Changchun 130022, China*

*<sup>a</sup>Information Technology College, Jilin Agricultural University, Changchun 130033, China*

2.3 $\mu$ m wavelength InGaAsSb/AlGaAsSb quantum-wells(QWs) diode lasers (LDs) had been fabricated and characterized, with cavity lengths of 1000  $\mu$ m and stripe width of 150 $\mu$ m. By carefully designing and realizing experimentally the active quantum-well region, the high output performance was achieved with the threshold current density of the device is as low as 339A/cm<sup>2</sup>. The vertical and parallel divergent angles were  $\theta_{\perp}=63^{\circ}$  and  $\theta_{\parallel}=31^{\circ}$ , respectively. The continuous wave operating up to 632 mW at room temperature (RT) was achieved.

(Received September, 29, 2014; accepted November 13, 2014)

**Keywords:** Continuous-wave (CW) operating, InGaAsSb/AlGaAsSb laser diodes (LDs), Room temperature (RT), Quantum-well (MBE)

## 1. Introduction

Semiconductor lasers emitting in the mid-infrared spectral region is of enormous interest as the practical realization of optoelectronic devices operating in the 2-4 $\mu$ m wavelength range, and offers potential applications in a wide variety of areas, e.g., ultra-sensitive laser spectroscopy, medical diagnostics, home security, industrial process monitoring, infrared countermeasures, optical wireless communications, etc. [1-7]. Laser diodes emitting at 2 $\mu$ m with the high beam quality and easy scaling of available output power could be considerably advantageous in the 1.8-2.8 $\mu$ m wavelength range owing to applications like the ideal as optical pumping sources for Ho-doped YAG solid-state lasers and for long-wavelength semiconductor lasers.

MIR GaSb operating in continuous wave (CW) at room temperature (RT) were first devices. which moreover, series fulfill all the requirements of Sb-based semiconductor laser device results, exhibit low laser thresholds, with improved output performance and excellent temperature characteristics, have been obtained owing to the laser structure design, materials optimization, and epitaxial growth [8-12]. However, unlike GaAs or InP based materials system, the realization of electro-optical confinement with oxidation of an Al-rich layer or ion implantation is not possible with GaSb-based materials. Moreover, p-type GaSb based exhibit poor conductivity and high free-carrier absorption losses which limits electrically-pumped p-n junction to pulsed operation at RT. Development of the highly efficient semiconductor diode

lasers operating in 2-4 $\mu$ m spectral region will significantly improve the performance of the many existing systems and enable new applications [13,14].

In this paper, the works focused on InGaAsSb/AlGaAsSb MQWs laser diodes with the wavelength of 2.3 $\mu$ m were introduced. We investigated the optimized growth conditions, laser structures design and doping characters of InGaAsSb/AlGaAsSb multiple QW lasers, which were grown by molecular beam epitaxy (MBE), and GaSb-based type-I diode lasers with up to 2.3 $\mu$ m wavelength was fabricated and characterized. The epitaxial layer structures were analyzed by Scanning electron microscope (SEM) and high-resolution x-ray diffraction (HRXRD), indicating excellent lattice matching and thus high crystalline quality.

## 2. Experiment

Fig. 1 is schematic energy-band diagram of the broadened waveguide 2.3 $\mu$ m wavelength InGaAsSb/AlGaAsSb diode lasers. The laser structures were grown on n-GaSb (Te doping) substrate by molecular beam epitaxy. Heavily doping sources with Be and Te to a concentration of  $3.0 \times 10^{18} \text{cm}^{-3}$  and  $2.0 \times 10^{18} \text{cm}^{-3}$ , respectively. The active region consists of three 10-nm-thickness  $\text{In}_{0.37}\text{Ga}_{0.63}\text{As}_{0.02}\text{Sb}_{0.98}$  quantum wells surrounded by  $\text{Al}_{0.35}\text{Ga}_{0.65}\text{As}_{0.03}\text{Sb}_{0.97}$  barriers, and 1.5% compressively strain existed in the quantum wells, 400nm undoped  $\text{Al}_{0.35}\text{Ga}_{0.65}\text{As}_{0.02}\text{Sb}_{0.98}$  lower waveguide layer and 400 nm  $\text{Al}_{0.35}\text{Ga}_{0.65}\text{As}_{0.03}\text{Sb}_{0.97}$  upper waveguide layer were

sequentially grown. High compositionally graded Al in cladding contributed to an improved resistance and crystal quality, was necessary to heavily n-type doped the cladding layer with Te and the lower refractive index for sufficient gain overlap and injection efficiency, while adding Al composition of  $>0.35$  in wells can increase the valence band offset for better hole confinement. 1.2- $\mu\text{m}$ -thick Te-doped  $\text{Al}_x\text{Ga}_{1-x}\text{As}_{0.07}\text{Sb}_{0.93}$  ( $0.35 \leq x \leq 0.9$ ) lower cladding layers and 1.2- $\mu\text{m}$ -thick Be-doped  $\text{Al}_x\text{Ga}_{1-x}\text{As}_{0.07}\text{Sb}_{0.93}$  ( $0.35 \leq x \leq 0.9$ ) upper cladding layer were grown. The Be-doped [ $2.0 \times 10^{19} \text{cm}^{-3}$ ] ohmic contact layers were grown.

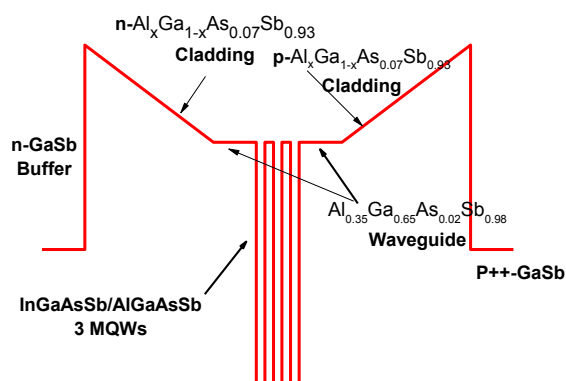


Fig. 1. Schematic energy-band diagram of the broadened waveguide 2.3 $\mu\text{m}$  wavelength InGaAsSb/AlGaAsSb diode lasers.

The InGaAsSb/AlGaAsSb laser structure with stripe width of 150- $\mu\text{m}$  and cavity length of 1000- $\mu\text{m}$  were fabricated, and contacts were defined using standard photolithography. The n-side of the wafer was thinned to a thickness of about 130 $\mu\text{m}$  by mechanical method. Conventional Ti-Pt-Au and Au-Ge-Ni contacts were evaporated as the top p- and n-contacts, respectively. After alloying, the laser facets were coated with anti-reflection (AR) and high reflection (HR) thin films, with reflection of 3% and 95%, reflectivity. The lasers were soldered on copper heat-sinks for heat dissipation.

### 3. Results and discussion

Mainly the high Indium content lead to the strain, which was increased to increase the wavelength, therefore all active regions exhibit a sufficient valence band offset, leading to a low threshold current density and over the entire wavelength to 2.3 $\mu\text{m}$ . For the optimizations of the MQWs interface, under appropriate parameters, indicating a smoothing of the sample surface achieved with layer by layer growth, the typical SEM micrograph of the quantum well had been shown in insert of Fig. 2. An experimental pattern, exhibited well-defined, narrow, intense peaks that reveal a very high crystalline quality with sharp interfaces. A satellite peak series corresponding to the well-barrier

periodicity appears clearly in Fig. 2. The X-ray diffraction (XRD) measurements confirmed all the layers were closely lattice matched to the GaSb substrate.

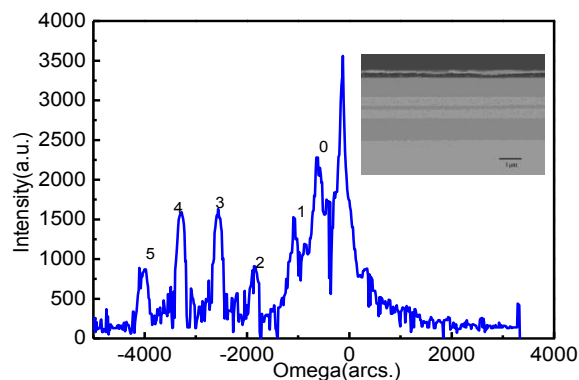


Fig. 2. The X-ray diffraction (XRD) measurements curve. Insert shows the typical SEM micrograph of the quantum well.

The output power versus current (L-I) characterization under CW operation at room temperature in Fig. 3, exhibited a low threshold of 632mA, equivalent to a threshold current density for the laser size of 150 $\mu\text{m}$  (stripe width)  $\times$  1000 $\mu\text{m}$  (cavity length), and a 4.2% maximum power conversion efficiency (PCE). The maximum output power is 632 mW at a drive current about 2.5A. The low threshold is attributed to the excellent crystalline quality and reduced the optical absorption of the injected free carriers in the QW layers. The insert shows the lasing emission spectra of the laser diode measured under CW operation at room temperature with the current of 1 A, both of which consist of multiple longitudinal modes. Laser central peak emission wavelength is around 2.3 $\mu\text{m}$  for 2.5A at room temperature.

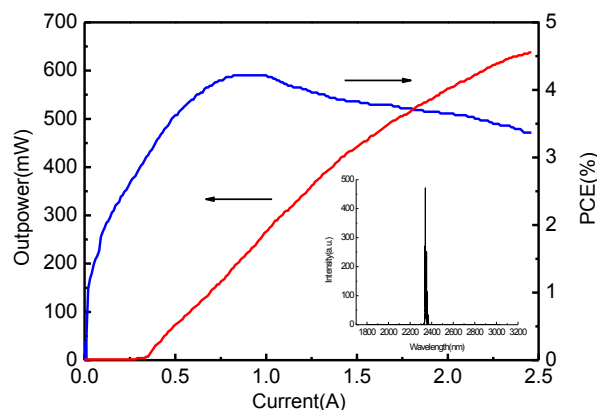


Fig. 3. CW output power and power conversion efficiency (PCE) versus current at room temperature. The insert shows the dependence of wavelength with the current of 1 A.

Fig. 4 shows that the device can produce narrow

far-field patterns, relatively far-field vertical and parallel divergent angles  $\theta_{\perp}=63^{\circ}$  and  $\theta_{\parallel}=31^{\circ}$  were achieved, respectively. High Al composition and appropriate waveguide thickness may lead to the beam divergence angle, a high confinement factor with the undoped cladding layers, enabling low internal losses. Further work to improve beam quality should focus on optimal designing, minimizing optical confinement factor, and decreasing internal loss.

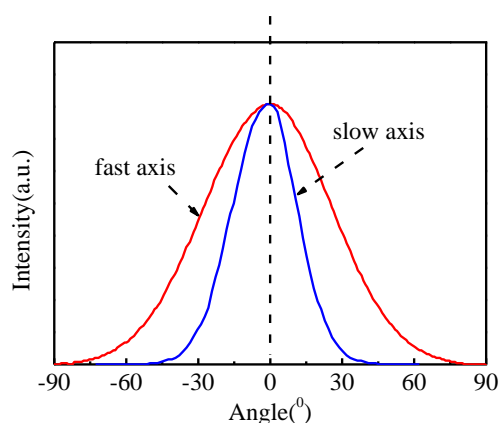


Fig. 4. The far-field vertical and parallel divergent angles with  $\theta_{\perp}=63^{\circ}$  and  $\theta_{\parallel}=31^{\circ}$ .

#### 4. Conclusions

In summary, we had fabricated room-temperature continuous wave operation of 2.3 $\mu\text{m}$  InGaAsSb/AlGaAsSb quantum-wells laser diode by MBE. The output performance was achieved with the threshold current densities of the device is as low as 339 A/cm<sup>2</sup>, the maximum output power 632 mW at a drive current about 2.5A, and vertical and parallel divergent angles  $\theta_{\perp}=63^{\circ}$  and  $\theta_{\parallel}=31^{\circ}$ , respectively.

#### Acknowledgements

This work was financially supported by the National Natural Science Foundation of China under Grant Nos 61370043, 60976056, 61308051 and 61006039, NSAF Nos U133306, Science Foundation of JiLin Province (20140520139JH), and Excellent Youth Doctor Foundation of Jilin Agricultural University(No.201411)

#### References

- [1] C. Lin, M. Grau, O. Dier, et al, Appl. Phys. Lett., **84**(25), 5088 (2004).
- [2] D. Donetsky, J. Chen, L. Shterengas, et al, J. of Electronic Materials, **37**, 12 (2008).
- [3] T. Hosoda, G. Belenky, L. Shterengas, et al, Appl. Phys. Lett., **92**, 091106 (2008).
- [4] L. Shterengas, G. Belenky, M. Kisi, Appl. Phys. Lett., **90**, 011119 (2007).
- [5] Jianfeng Chen, Dmitry Donetsky, Leon Shterengas, et al, IEEE Photon. Techn. Lett., **44**, 12 (2008).
- [6] H. K. Choi, S. J. Eglash, Appl. Phys. Lett., **61**, 1154 (1992).
- [7] R. Colombelli, F. Capasso, C. Gmachl et al. Appl. Phys. Lett., **78**, 2620 (2001).
- [8] J. G. Kim, L. Shterengas et al. Appl. Phys. Lett. **81**, \ 3146 (1992).
- [9] J. G. Kim, L. Shterengas, R. U. Martinelli, et al, Appl. Phys. Lett., **83**, 1926 (2003).
- [10] M. Rattunde\*a, E. Geerlingsa, J. Schmitza, et al, SPIE **5738**, 138 (2014).
- [11] D. Z. Garbuzov, R. U. Martinelli, H. Lee, et al. Appl. Phys. Lett., **70**, 2931 (1997).
- [12] Wen Lei, Chennupati Jagadish, Journal of Applied Physics **104**, 091101 (2008).
- [13] B. Rodriguez, L. Cerutti, E. Tournié, Appl. Phys. Lett., **94**, 023506 (2009).
- [14] T. Hosoda, G. Kipshidze, L. Shterengas, Gregory Belenky, Appl. Phys. Lett., **94**, 261104 (2009).

\*Corresponding author: mhyou000@126.com;

lzhg000@126.com